X-ray Structure Refinement of (3 + 1)-Dimensional Incommensurate Composite $(1 - x)\mathrm{Ta_2O_5}.x\mathrm{WO_3}$, $x = 0.1$

Siegbert Schmid,* Klaus Fütterer and John G. Thompson

Research School of Chemistry, Australian National University, Canberra ACT 0200, Australia

Abstract

The structure refinement of tantalum tungstate, $(1 - x)\mathrm{Ta_2O_5}.x\mathrm{WO_3}$, $x = 0.1$, as a $(3 + 1)$-dimensional incommensurately modulated composite structure was carried out using X-ray single-crystal diffraction data measured with Mo $K\alpha$ radiation. The composite structure consists of two component substructures referred to as the metal-substructure (M), $a_M = 6.188\,(1)$, $b_M = 3.665\,(1)$, $c_M = 3.886\,(1)\,\mathrm{\AA}$, and the oxygen-substructure (O), $a_O = a_M$, $b_O = 2.251\,\mathrm{\AA} = b_M/1.628$, $c_O = c_M$, respectively. The primary modulation wavevector of the M substructure is chosen to be $\mathbf{q}_M = \mathbf{b}_O^* = 1.628\,\mathbf{b}_M^*$. The overall superspace-group symmetry is $C'mmm(0\beta0)s00$. The structure was refined to an overall $wR = 0.0561$. The structures of the compounds $x = 0.267$ $(\mathrm{Ta_{22}W_4O_{67}})$ and $x = 0.14$ $(\mathrm{Ta_{74}W_6O_{203}})$, also members of the $(1 - x)\mathrm{Ta_2O_5}.x\mathrm{WO_3}$, $0 \leq x \leq 0.267$, solid solution, were rerefined as incommensurately modulated structures using intensity data reported previously. The displacive modulation wave amplitudes obtained from these refinements are in remarkable agreement with each other. Beyond the similarity of the atomic modulation functions across the solid solution, the structures show subtle but significant differences as a function of composition in the following ways: displacement of atom O_M along the **b** direction and both bond-valence sum and thermal parameter mean-square displacement along **c** of the metal atom.

1. Introduction

The solid solution $(1 - x)\mathrm{Ta_2O_5}.x\mathrm{WO_3}$, $0 \leq x \leq 0.267$, has been subject to intensive investigation over many years (see Schmid *et al.*, 1995, for a review). Stephenson & Roth (1971*a,b,c,d*) published four structures within the above solid solution field and described them as belonging to an infinite series of anion-deficient α-$\mathrm{UO_3}$-related 'line phases'. Recently, the structures of $\mathrm{Ta_{22}W_4O_{67}}$ $(x = 0.267)$ and $\mathrm{Ta_{74}W_6O_{203}}$ $(x = 0.140)$ have been refined as commensurately modulated

structures, corresponding to 13 and 8 times super-structures, respectively, of the α-$\mathrm{UO_3}$-related metal ion array (Schmid *et al.*, 1995; Rae, Schmid, Thompson, Withers & Ishizawa, 1995). These refinements show that the whole solid solution can be represented by the same set of periodic atomic modulation functions (AMFs) when described as a composite modulated structure using the $(3 + 1)$-dimensional superspace approach (Janner & Janssen, 1980; van Smaalen, 1991; Yamamoto, 1992, 1993). The structural analysis (Rae, Schmid, Thompson, Withers & Ishizawa, 1995), however, left some ambiguity concerning the commensurateness or incommensurateness of the two component substructures. The algorithm used for the evaluation of the structure factor expression required a three-dimensional space-group symmetry for each composition ($C112/m$ for $\mathrm{Ta_{22}W_4O_{67}}$ and $Pbam$ for $\mathrm{Ta_{74}W_6O_{203}}$). Thus, the description of the structures was actually restricted to a commensurate modulation. Yet, refinement as an incommensurately modulated structure is the more general approach for such a solid solution and it is desirable that the structure refinement should not be restricted by assuming the validity of a three-dimensional space-group symmetry. As it is possible to synthesize single crystals at any composition within the solid solution, implying a continuous range of values for the modulus of the primary modulation wavevector (see Schmid, Withers & Thompson, 1992), it would be necessary for some compositions to invoke improbably large supercells (with respect to the metal parent cell) to allow a commensurate description. For example, the composition studied in the present work, with $\mathbf{q}_M = 1.628\,\mathbf{b}_M^*$, would require a 43 times supercell.

Thus, X-ray diffraction intensity data of a single crystal of composition $x = 0.1$, with primary modulation wavevector $\mathbf{q}_M = 1.628\,\mathbf{b}_M^*$, were recorded and refined as an incommensurately modulated structure. To facilitate comparison of the $x = 0.1$ structure with $\mathrm{Ta_{22}W_4O_{67}}$ and $\mathrm{Ta_{74}W_6O_{203}}$, these latter structures were rerefined using the previously reported data (Schmid *et al.*, 1995; Rae, Schmid, Thompson, Withers & Ishizawa, 1995), but this time as an incommensurately modulated structure and are presented here together with the new data of the $x = 0.1$ sample.

Table 1. *Parameters of intensity data collection*

Diffractometer	Philips PW1100/20
	Software amendments by Grigg & Barnea (1993)
Radiation	Mo $K\alpha$, Graphite monochromator
Scan mode	$2\theta/\omega$-scan, $\Delta\omega = 1.5° + 0.35\tan\theta$
Scan speed (° min⁻¹)	1.5
Data collection	$4 \leq 2\theta \leq 60$
limits in 2θ (°),	$-8 \leq h \leq 8$
$hklm$	$-9 \leq k \leq 9$
	$-5 \leq l \leq 5$
	$-7 \leq m \leq 7$
No. of measured reflections	7544; unique: 1105; unique with $F^2 \geq 3\sigma(F^2)$: 782
Standards	3 reflections, monitored every 120 min: 201, 222, 020
Lattice parameters (Å)	6.188(1), 3.665(1), 3.886(1) (orthorhombic)
	determined from 25 reflections, $13 \leq 2\theta \leq 34°$
Modulation wavevector	$q_M = (1.628 \pm 0.001) b_M^*$, determined from centring 15 satellite reflections
Lorentz–polarization correction	*Xtal*3.0 (Hall & Stewart, 1990)
Absorption correction	Empirical absorption correction, *RAELS*94 (Rae, 1994)

2. Experimental

2.1. *Synthesis*

Single crystals of $(1-x)Ta_2O_5.xWO_3$, $x = 0.1$, were grown according to procedures described previously (Schmid, Withers & Thompson, 1992; Schmid *et al.*, 1995).

2.2. *Intensity measurement and data processing*

For $(1-x)Ta_2O_5.xWO_3$, $x = 0.267$ and 0.140, data sets were used that had been collected on Beamline 14A at the Photon Factory, Tsukuba, Japan. All details on these data sets are given elsewhere (Schmid *et al.*, 1995; Rae, Schmid, Thompson, Withers & Ishizawa, 1995).

For the intensity measurement on $(1-x)Ta_2O_5.xWO_3$, $x = 0.1$, a crystal was selected approximately ellipsoidal in shape with dimensions $0.1 \times 0.05 \times 0.05$ mm³. Accurate lattice parameters for the underlying metal parent subcell (see Table 1) were obtained from a least-squares fit of the setting angles for 25 reflections with 2θ values between 13 and 34° using Mo $K\alpha$ radiation on a Philips PW1100/20 diffractometer.

In the next step the magnitude of the primary modulation wavevector characteristic of the metal or M substructure was established to be $q_M = 1.628 b_M^*$ by carefully centring 15 satellite reflections. The data collection was performed in parts. The parent and various orders of satellite reflections were collected separately using software that was developed to enable data collection on incommensurately modulated crystals on a Philips PW1100/20 diffractometer (Grigg & Barnea, 1993).

Background counting time was 10 s on either side of the scan. Square slits subtended angles $1 \times 1°$ at the crystal. The Lorentz–polarization correction was performed using the program package *Xtal*3.0 (Hall & Stewart, 1990). An empirical absorption correction was applied using *RAELS*94 (Rae, 1994). The three standard reflections measured every 120 min showed a significant

linear decrease in intensity of $\sim 4.5\%$ throughout the 3 weeks of data collection due to decreasing tube intensity. After correcting the data for this decrease in standard reflection intensities no unusual features were left. Averaging the reflection intensities in Laue symmetry *mmm* gave 782 unique reflections (internal $R = 0.059$ on F^2) with $F^2 \geq 3\sigma(F^2)$. Other important parameters for the data collection are given in Table 1.*

3. Symmetry

The symmetry of the $(1-x)Ta_2O_5.xWO_3$ solid solution in terms of a compositely modulated structure using the superspace approach (Janner & Janssen, 1980; van Smaalen, 1991; Yamamoto, 1992, 1993) has been presented at length in Rae, Schmid, Thompson, Withers & Ishizawa (1995). Therefore, only the facts relevant to the refinement are summarized below.

(1) The $(1-x)Ta_2O_5.xWO_3$ solid solution can be regarded as a $(3+1)$-dimensional composite modulated structure, consisting of two subsystems – a metal ion or M subsystem and an oxygen ion or O subsystem. The M substructure comprises the α-UO_3-related metal-atom array, as well as the oxygens located at the apices (labelled O_M) of the metal-atom coordination polyhedra. The latter vary between octahedral and pentagonal bipyramidal. The O substructure is formed by the oxygen ion array located in the basal plane of the metal coordination polyhedra. While the **a** and **c** axes of the two subsystems are the same, the **b** lattice parameters are mutually incommensurable. The lattice parameters of the sample with composition $x = 0.1$ were

$$M : a_M = a = 6.188(1), \quad b_M = 3.665(1), \quad c_M = c = 3.886(1)\,\text{Å}$$
$$O : a_O = a_M \qquad\qquad b_O = 2.251\,\text{Å} = b_M/1.628, c_O = c_M.$$

(2) The primary modulation wavevector of the metal subsystem was chosen to be $q_M = b_O^* = 1.628 b_M^*$.

(3) The matrix W (see van Smaalen, 1991), transforming the metal-ion subsystem into the oxygen-ion subsystem, is then given by

$$W = \begin{pmatrix} 1 & 0 & 0 & 0 \\ 0 & 0 & 0 & 1 \\ 0 & 0 & 1 & 0 \\ 0 & 1 & 0 & 0 \end{pmatrix}, \text{ with } (\mathbf{a}^*, \mathbf{b}^*, \mathbf{c}^*, \mathbf{q})_O$$
$$= (\mathbf{a}^*, \mathbf{b}^*, \mathbf{c}^*, \mathbf{q})_M W^T,$$

where W^T is the transposed matrix.

(4) With the above choice of primary modulation wavevector, the extinction conditions characteristic of the whole solid solution field are $F(hklm) = 0$ unless $h + k + m = 2n$ and $F(0klm) = 0$ unless $k, m = 2n$. The

---

Table 2. *Relevant parameters of the refinements*

Compound	$Ta_{22}W_4O_{67}$ ($x = 0.267$)		$Ta_{74}W_6O_{203}$ ($x = 0.140$)		$(1-x)Ta_2O_5.xWO_3$ ($x = 0.1$)	
Intensity data sets	taw4n	taw4f	taw6n		tawic	
Wavelength (Å)	1.2563	1.2741	1.2563		Mo$K\alpha$	
Energy difference to TaL_{III} edge (eV)	8	146	8			
Primary modulation wavevector $q = \beta b_M^*$	$\beta = 1.615$		$\beta = 1.625$		$\beta = 1.628$	
Overall symmetry			$C'mmm(0\beta0)s00$			
Symmetry of commensurate superstructure	$C112/m$ ($b' = 13 b_M$)		$Pbam$ ($b' = 8 b_M$)			
No. of refined parameters	52, 50	52	54, 52		47	
No. of unique reflections, $R(F^2)_{merge}$						
$F^2 \geq 3\sigma(F^2)$ all	420	4.10	895	4.95	1124	2.92	782	5.89
$m = 0$	41	2.21	86	3.05	104	3.01	92	2.96
$m = 1$	58	2.32	119	2.91	151	2.90	118	6.67
$m = 2$	71	1.80	146	2.37	176	2.65	145	4.49
$m = 3$	58	2.08	122	2.83	155	2.63	129	4.49
$m = 4$	69	10.02	138	8.87	167	2.89	105	9.94
$m = 5$	55	13.20	115	14.60	138	3.16	93	9.48
$m = 6$	58	16.44	129	19.90	144	3.31	76	13.68
$m \geq 7$	10	70.21	40	25.39	89	6.22	24	26.70
Extinction correction			Type I, Lorentz distribution			
Weight	Unit	Unit	Unit		$1/\sigma^2(F)$	

former condition implies a non-standard centring in superspace of the form $\{1|\frac{1}{2},\frac{1}{2},0,\frac{1}{2}\}$, which will be indicated by the label C'. The latter requires the presence of a glide plane $\{\sigma_x|0,0,0,\frac{1}{2}\}$. The superspace group, therefore, has at least $C'm-(0\beta0)s--$ symmetry, but is most likely $C'mmm(0\beta0)s00$. In fact, this superspace group was chosen for the refinement.

(5) The origin in the fourth dimension was fixed by the superspace symmetry operation $\{i|0,0,0,0\}$.

(6) The M substructure AMFs describing the displacive $(u_{\mu i}(t_M); i = x, y, z)$, occupational $(\Delta P_\mu(t_M))$ and anisotropic thermal parameter deviations $(\Delta U_{ij}^\mu(t_M),$ $i, j = 1, 2, 3)$ from their average values as a function of $q_M \cdot t_M$ are given by

$$u_{\mu x}(t_M) = \sum_{2n+1} a_{\mu x}([2n+1]q_M)\sin(2\pi[2n+1]q_M \cdot t_M)$$
$$\mu = \text{Ta/W}, \text{O}_M$$

$$u_{\mu y}(t_M) = \sum_{2n} a_{\mu y}(2nq_M)\sin(2\pi \cdot 2nq_M \cdot t_M)$$
$$\mu = \text{Ta/W}, \text{O}_M$$

$$\Delta U_{ii}^\mu(t_M) = \sum_{2n} U_{ii}^\mu(2nq_M)\cos(2\pi \cdot 2nq_M \cdot t_M)$$
$$\mu = \text{Ta/W}, \text{O}_M, i = 1, 2, 3$$

$$\Delta U_{12}^\mu(t_M) = \sum_{2n+1} U_{xy}^\mu([2n+1]q_M)\cos(2\pi[2n+1]q_M \cdot t_M)$$
$$\mu = \text{Ta/W}, \text{O}_M$$

$$\Delta P_\mu(t_M) = \sum_{2n} P_\mu(2nq_M)\cos(2\pi \cdot 2nq_M \cdot t_M)$$
$$\mu = \text{Ta/W}, \text{O}_M,$$

where $n = m_M$ is an integer which labels the harmonic order of the corresponding modulation wave with respect to the M substructure. Note that for $u_{\mu x}(t_M)$ the AMF was changed from a cosine to a sine function with respect to Rae, Schmid, Thompson, Withers & Ishizawa (1995) due to the origin choice stated above. The corresponding O substructure AMFs are given by

$$u_{Ox}(t_O) = \sum_{2n+1} a_{Ox}([2n+1]q_O)\cos(2\pi[2n+1]q_O \cdot t_O),$$

$$u_{Oy}(t_O) = \sum_{2n} a_{Oy}(2nq_O)\sin(2\pi \cdot 2nq_O \cdot t_O)$$

$$\Delta U_{ii}^O(t_O) = \sum_{2n} U_{ii}^O(2nq_O)\cos(2\pi \cdot 2nq_O \cdot t_O), \quad i = 1,2,3$$

$$\Delta U_{12}^O(t_O) = \sum_{2n+1} U_{xy}^O([2n+1]q_O)\sin(2\pi[2n+1]q_O \cdot t_O).$$

Here $n = m_O$ is an integer which labels the harmonic order of the corresponding modulation wave with respect to the O substructure. The position R_μ of an atom μ in the modulated structure is then described by $R_\mu = r_\mu + t + u_\mu(r_\mu + t)$, where r_μ is the average position in the asymmetric unit and t is a Bravais lattice vector of the respective substructure. Similarly, the thermal parameter tensor is given by $U_{ij}^\mu(q \cdot t) = U_{ij}^\mu + \Delta U_{ij}^\mu(t)$ and the occupation probability by $P_\mu(q \cdot t) = P_\mu + \Delta P_\mu(t)$.

The average positions with respect to the underlying parent substructure are Ta/W $(0,0,0)$, O_M $(0,0,\frac{1}{2})$ and O $(\frac{1}{4},\frac{1}{4},0)$.

Note that the superspace-symmetry operation $\{\sigma_z|0000\}$ forbids displacive modulation along c for either substructure. The possibility of lowering the overall superspace-group symmetry to a $C'm-(0\beta0)s--$ subgroup of $C'mmm(0\beta0)s00$ was carefully considered, but not found to be justified.

4. Structure refinements

The refinements carried out on the four intensity data sets listed in Table 2 were labelled taw4n, taw4f, taw6n and tawic corresponding to the compounds $x = 0.267$ ($Ta_{22}W_4O_{67}$), $x = 0.14$ ($Ta_{74}W_6O_{203}$) and $x = 0.1$ ('incommensurate'), respectively. The suffixes 'f' and 'n' refer to the data recorded at the synchrotron and correspond to 'far' and 'near' to the TaL_{III} absorption edge, respectively. The data with suffix 'n' thus possess an enhanced scattering contrast between Ta and W and

Table 3. Refinement statistics

Compound	$Ta_{22}W_4O_{67}$ ($x = 0.267$)			$Ta_{74}W_6O_{203}$ ($x = 0.140$)		$(1-x)Ta_2O_5.xWO_3$ ($x = 0.1$)
Label of refinement runs	taw4n-20	taw4n-32	taw4f-10	taw6n-26	taw6n-27	tawic-30
Occupational modulation refined	Yes	No	No	Yes	No	No
Wavelength (Å) (ΔE to TaL_{III}, e V)	1.2563 (8)		1.2741 (146)	1.2563 (8)		Mo $K\alpha$
$R(F)$, $wR(F)$						
all	3.40	3.85	5.34	7.57	7.57	8.00, 5.61
$m = 0$	1.75	1.83	2.27	3.43	3.42	3.77, 3.98
$m = 1$	4.25	3.71	4.76	9.00	8.92	12.93, 12.53
$m = 2$	2.64	4.14	4.30	6.06	6.11	5.96, 6.57
$m = 3$	2.29	2.31	2.75	5.55	5.53	7.22, 6.27
$m = 4$	6.11	8.81	9.48	11.10	11.50	10.32, 8.05
$m = 5$	7.01	7.24	8.78	9.52	9.49	15.62, 16.81
$m = 6$	11.08	10.95	24.62	15.65	15.50	14.51, 12.56
$m \geq 7$	80.03	79.93	63.58	40.20	39.06	32.53, 36.98

Table 4. Displacive Fourier terms of the atomic modulation function

Refinement	$Ta_{22}W_4O_{67}$ ($x = 0.267$) taw4n-20	taw4f-10	$Ta_{74}W_6O_{203}$ ($x = 0.14$) taw6n-26	$(1-x)-$ $Ta_2O_5.xWO_3$ ($x = 0.1$) tawic-30
W $P(2q_M)$	0.27 (2)	0.0	0.06 (3)	0.0
W $P(4q_M)$	0.10 (2)	0.0	0.05 (3)	0.0
Ta/W $a_x(q)$	0.0338 (2)	0.0343 (1)	0.0360 (2)	0.0372 (2)
$a_x(3q)$	−0.0411 (2)	−0.0411 (2)	−0.0449 (2)	−0.0436 (2)
$a_x(5q)$	0.0002 (2)	0.0003 (2)	−0.0007 (2)	−0.0002 (3)
$a_x(7q)$	−0.0008 (4)	0.0002 (3)	−0.0053 (2)	−0.0027 (4)
$a_y(2q)$	0.0323 (2)	0.0329 (2)	0.0375 (2)	0.0392 (4)
$a_y(4q)$	−0.0025 (2)	−0.0020 (2)	−0.0021 (2)	−0.0019 (6)
$a_y(6q)$	−0.0022 (2)	−0.0017 (2)	−0.0034 (3)	−0.0038 (7)
$a_y(8q)$	0.0018 (3)	0.0023 (3)	−0.0006 (3)	0.0019 (9)
O_M $a_x(q)$	0.053 (1)	0.053 (2)	0.052 (2)	0.044 (3)
$a_x(3q)$	−0.027 (1)	−0.027 (2)	−0.032 (2)	−0.032 (3)
$a_x(5q)$	−0.001 (2)	0.000 (2)	0.002 (2)	0.005 (5)
$a_y(2q)$	0.067 (2)	0.067 (3)	0.067 (3)	0.066 (6)
$a_y(4q)$	0.002 (2)	0.004 (3)	0.012 (3)	0.033 (8)
$a_y(6q)$	−0.002 (2)	−0.001 (3)	0.003 (3)	0.02 (1)
O $a_x(q)$	0.126 (1)	0.125 (1)	0.128 (1)	0.128 (2)
$a_x(3q)$	0.016 (1)	0.015 (1)	0.015 (1)	0.012 (2)
$a_x(5q)$	0.038 (1)	0.038 (1)	0.045 (1)	−0.045 (2)
$a_x(7q)$	−0.001 (1)	−0.001 (2)	−0.001 (1)	−0.001 (3)
$a_y(2q)$	−0.138 (3)	−0.141 (3)	−0.142 (3)	−0.149 (6)
$a_y(4q)$	−0.008 (3)	−0.004 (3)	−0.004 (3)	−0.002 (7)
$a_y(6q)$	0.005 (3)	0.005 (3)	0.002 (3)	−0.002 (8)

are appropriate to distinguish both atoms in a structure refinement. Table 2 summarizes the important numbers for the different refinements, while Table 3 displays the resulting residual values.

The refinements were carried out using the software package *JANA94* (Petřicek, 1994) minimizing the function $wR = \{\sum w(|F_o| - |F_c|)^2 / \sum w|F_o|^2\}^{1/2}$. Initially all displacive Fourier terms were set to zero, except the three low-order displacive parameters $a_{Mx}(q_M)$, $a_{Mx}(3q_M)$ and $a_{My}(2q_M)$, which were refined together with the scale factor from starting values ±0.01. This was done since it was plausibly assumed that the scattering contribution of the metal atoms predominantly determines the relative phases of the displacive coefficients (see Rae, Schmid, Thompson, Withers & Ishizawa, 1995). The signs of these coefficients were systematically varied and the sign combination corresponding to the true minimum was marked by a distinct drop of the

residual values. From there on the displacive parameters of the atoms O and O_M were released from near-zero starting values, i.e. 0.0001, in a hierarchical refinement procedure with stepwise increasing Fourier term order. At this stage displacive terms up to fourth order were released for atoms M, O_M and up to fifth order for O.

The next crucial steps in order to obtain a satisfactory fit were to introduce thermal parameter modulation for the metal atoms including terms up to fourth order and an extinction correction. The release of higher than fifth-order displacive terms and thermal parameter modulation parameters up to second order for both O and O_M gave only a marginal improvement of the overall fit and had most impact on the fit of the higher-order satellite reflections.

The data taw4n and taw6n were used to refine the occupational modulation of Ta and W (see columns 'taw4n-20' and 'taw6n-26' in Table 3). In order to test the impact of the corresponding parameters $P_\mu(2nq_M)$ on the fit, the same data were also refined setting these values to zero (see columns 'taw4n-32' and 'taw6n-27' in Table 3).

5. Results and discussion

5.1. Refinement statistics

The structural parameters resulting from the refinement of $(1-x)Ta_2O_5.xWO_3$, $x = 0.1$, 0.267 ($Ta_{22}W_4O_{67}$) and 0.14 ($Ta_{74}W_6O_{203}$), are given in Tables 4 (Fourier coefficients of the displacive modulation) and 5 (thermal parameters and corresponding Fourier coefficients). The AMFs of the $x = 0.1$ sample are plotted in Fig. 1, while Fig. 2 displays the displacement along the b direction as a function of $q \cdot t$ of atom O_M for all three compounds.

The comparison of the residual values of the different refinements is difficult, due to substantial differences in the number of available intensity data points (owing to the constraints of beam time allocation at the synchrotron as well as to the different 2θ ranges, giving measurable Bragg intensity on the synchrotron compared with the sealed tube). From the data compiled in Table 2 it is apparent that the intensity data recorded at the

synchrotron show distinctly lower R values on averaging symmetry-equivalent reflections than those recorded using in-house equipment. This is mainly due to the difference in size of the crystal used for the measurement, since the much more intense synchrotron source allowed the choice of a smaller crystal ($\sim 10\,\mu m$ in diameter), implying a reduction of absorption and extinction problems. Yet the refinements of the $x = 0.1$ sample and of $Ta_{74}W_6O_{203}$, which are close in composition, show rather similar agreement indices, apart from the first-order satellite reflections. The unsatisfactory fit to the first-order satellite reflections compared with the main, second- and third-order satellite reflections is, however, a common feature of all the refinements, although most pronounced in the case of the $x = 0.1$ sample. This will be discussed later. The best fit in terms of agreement indices was obtained for $Ta_{22}W_4O_{67}$ with
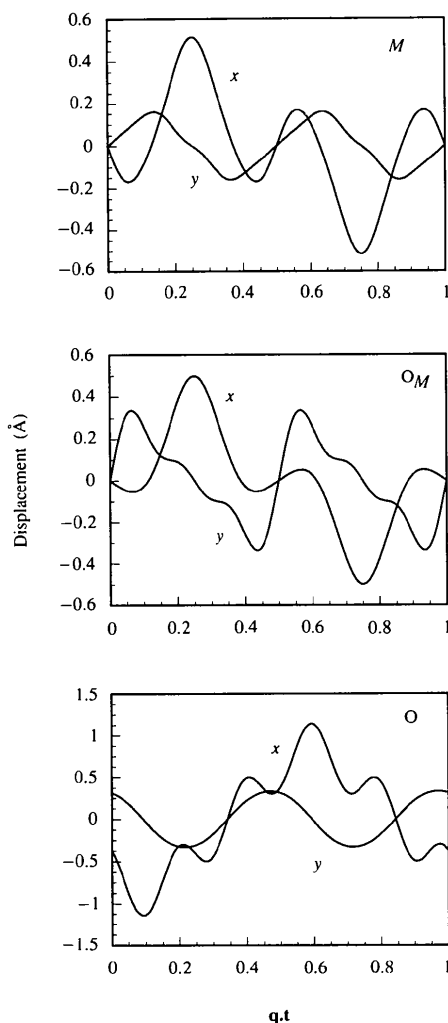

Fig. 1. Displacive atomic modulation functions of $(1 - x)Ta_2O_5{\cdot}xWO_3$, $x = 0.1$, as a function of $q \cdot t$.

Table 5. *Average thermal parameters and Fourier coefficients of the thermal atomic modulation functions*

Refinement	$Ta_{22}W_4O_{67}$ ($x = 0.267$)		$Ta_{74}W_6O_{203}$ ($x = 0.14$)	$(1-x)$-$Ta_2O_5{\cdot}xWO_3$ ($x = 0.1$)
	taw4n-20	taw4f-10	taw6n-26	tawic-30
Occupational modulation refined	Yes	No	Yes	No
Ta/W U_{11}	0.0164 (5)	0.0135 (3)	0.0094 (3)	0.0092 (4)
U_{22}	0.0082 (5)	0.0053 (2)	0.0086 (3)	0.0095 (4)
U_{33}	0.0249 (8)	0.0211 (3)	0.0254 (4)	0.0161 (4)
$U_{12}(q_M)$	0.0033 (3)	0.0035 (3)	0.0048 (3)	0.0049 (5)
$U_{11}(2q_M)$	-0.0020 (6)	-0.0027 (4)	-0.0022 (5)	-0.0015 (6)
$U_{22}(2q_M)$	-0.0003 (5)	-0.0015 (3)	0.0001 (5)	0.0021 (6)
$U_{33}(2q_M)$	0.0218 (8)	0.0247 (4)	0.0129 (6)	0.0088 (8)
$U_{12}(3q_M)$	-0.0045 (3)	-0.0034 (3)	-0.0033 (3)	-0.0037 (5)
$U_{11}(4q_M)$	-0.0010 (7)	-0.0013 (5)	-0.0075 (6)	-0.0043 (8)
$U_{22}(4q_M)$	-0.0016 (5)	-0.0024 (3)	-0.0031 (5)	-0.0046 (8)
$U_{33}(4q_M)$	0.0119 (8)	0.0128 (4)	0.0064 (6)	0.0030 (9)
O_M U_{11}	0.011 (3)	0.017 (4)	0.017 (3)	0.017 (6)
U_{22}	0.018 (4)	0.022 (3)	0.020 (3)	0.019 (7)
U_{33}	-0.001 (4)	-0.002 (3)	0.002 (2)	-0.001 (5)
$U_{12}(q_M)$	0.003 (4)	0.008 (4)	0.009 (4)	0.011 (9)
$U_{11}(2q_M)$	-0.001 (4)	0.009 (5)	0.001 (4)	0.00 (1)
$U_{22}(2q_M)$	0.010 (4)	0.013 (5)	0.013 (4)	-0.02 (1)
$U_{33}(2q_M)$	0.001 (5)	-0.009 (3)	0.001 (3)	0.01 (1)
O U_{11}	0.007 (2)	0.016 (3)	0.004 (2)	0.018 (6)
U_{22}	0.007 (2)	0.009 (2)	0.009 (2)	0.004 (5)
U_{33}	0.020 (4)	0.010 (3)	0.016 (2)	0.001 (4)
$U_{12}(q_M)$	-0.004 (3)	-0.005 (3)	-0.006 (2)	0.0
$U_{11}(2q_M)$	0.001 (3)	0.003 (4)	-0.002 (2)	0.005 (8)
$U_{22}(2q_M)$	-0.010 (3)	-0.013 (3)	-0.008 (3)	-0.010 (8)
$U_{33}(2q_M)$	-0.002 (5)	-0.000 (3)	-0.003 (3)	0.03 (7)

slight differences of 1.0% for main and low-order, *i.e.* first to third, satellite reflections, and up to 2% for the fourth- and fifth-order satellite reflections between the 'far' and the 'near' edge intensity data. Higher discrepancies than that are only seen for the generally very weak sixth and higher-order satellite reflections. These differences between taw4n and taw4f are very likely to be attributable to the difference in the number of measured reflections.

The residual values obtained from the refinements of $Ta_{22}W_4O_{67}$ and $Ta_{74}W_6O_{203}$ are in close agreement with those obtained by refining these compounds as commensurately (rather than incommensurately) modulated structures (Rae, Schmid, Thompson, Withers & Ishizawa, 1995). Since Rae, Schmid, Thompson, Withers & Ishizawa (1995) used a different approach to calculate structure factors (*i.e.* the structure factor expression was still based on individual atoms although refining Fourier coefficients of a modulation function), as well as allowing for corrections for twinning (in the case of $Ta_{22}W_4O_{67}$) and disorder (both compounds), the comparison has to be restricted to Model 2 of Rae, Schmid, Thompson, Withers & Ishizawa (1995), which is the most similar to our structural model. Yet, the agreement is remarkable both in terms of residual values and of displacive Fourier coefficients, which agree within three times the e.s.d.

5.2. The atomic modulation functions

The periodic displacements of the atoms as a function of $q \cdot t$ displayed in Fig. 1 represent the atomic displacement pattern for the whole solid solution, with the exception only of the **b** component of atom O_M. The latter is plotted for the three different compounds in Fig. 2. The description of the structures of different members of a solid solution series by one atomic modulation function is now well established and was shown to apply to very different systems, such as $(ZrN_{1-\Delta/2}F_{\Delta/2})F_{1+\Delta}$ (Schmid & Withers, 1995), $Nb_2Zr_{x-2}O_{2x+1}$ (Fütterer et al., 1995), and in the case of the present system by Schmid, Withers & Thompson (1992) and Rae, Schmid, Thompson, Withers & Ishizawa (1995). It is further confirmed by the present refinement with its high level of agreement between different compositions. However, beyond the similarity shown by the three members of the $(1-x)Ta_2O_5.xWO_3$ solid solution presented in this article, subtle but significant differences were revealed by the present comparative refinement of the $x = 0.1$ sample with the $x = 0.267$ and $x = 0.14$ compounds. This concerns the **b** component of the AMF of O_M as well as the thermal parameter modulation along the **c**
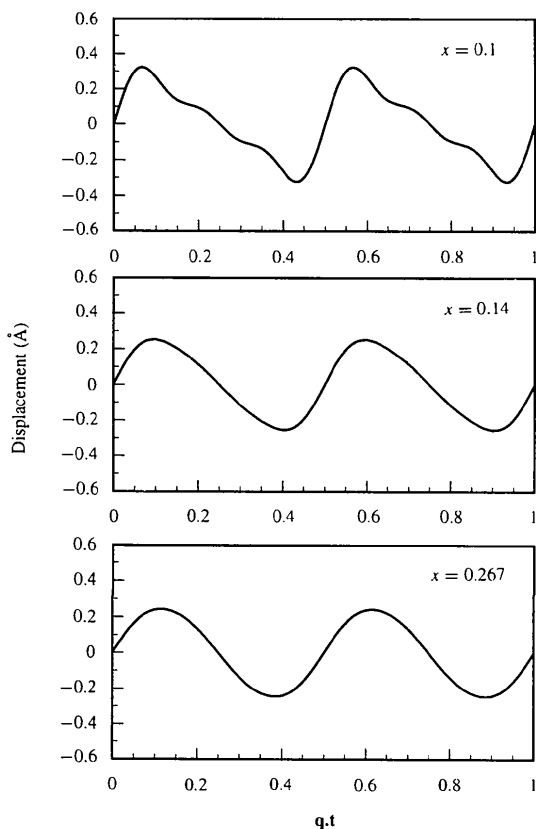

Fig. 2. The **b** component of the displacive atomic modulation function of atom O_M for different compositions.

direction of the metal atoms. The latter is discussed in §5.4.

The change in $a_y(4q_M)$ of O_M from near zero to 0.033 (8) on going from $x = 0.267$ (i.e. $Ta_{22}W_4O_{67}$) to $x = 0.1$ (see Table 4) is responsible for the continuous change of the y displacement from a sinusoidal to a sawtooth shape (see Fig. 2). This change is in turn responsible for the change of the $q \cdot t$-dependence of the average bond-valence sum of O_M displayed in Fig. 5 (see §5.4).

5.3. The coordination sphere

Fig. 6 shows a plot of metal–oxygen distances versus $t' = q_M \cdot (t_M - t_O)$ [distances and average bond valence sums were calculated using the software MISTEK (van Smaalen, 1994)]. Only oxygens situated in the basal plane are included as the apical oxygens O_M belong to the metal subsystem. Each curve in the plot corresponds to the distance variation of a specific metal–oxygen pair with t'. Due to the model of two interpenetrating and mutually incommensurable substructures, the relative origin of which changes continuously, the distance between a specific metal–oxygen pair goes from infinity to a minimum value and again to infinity for t' going from $-\infty$ to $+\infty$. By picking up all relevant metal–oxygen pairs in the coordination sphere of M and plotting them on top of each other one obtains an intuitive picture of the variation of the metal coordination number with t'.

The points at $t' = 0$ and $\frac{1}{2}$ show a fourfold coordination in the basal plane, resulting in a near exact octahedral coordination polyhedron when taking the apical O_M's into account. At the points in between, the basal plane coordination continuously varies between five- and fourfold, i.e. between a pentagonal bipyramidal and an octahedral coordination polyhedron. This consideration is, of course, fully equivalent to the corresponding discussion of the metal coordination polyhedra given in Schmid et al. (1995) in terms of the conventional superstructure description of $Ta_{22}W_4O_{67}$ and $Ta_{74}W_6O_{203}$.

5.4. Metal ordering

The refinement of metal-ion ordering in terms of an occupational modulation of the metal-atom site was carried out for $x = 0.267$ ($Ta_{22}W_4O_{67}$) and 0.14 ($Ta_{74}W_6O_{203}$) using the intensity data sets taw4n and taw6n, which possess an increased scattering contrast between Ta and W. While the release of the corresponding parameters $P_\mu(2q_M)$ and $P_\mu(4q_M)$ resulted in values significantly different from zero, as well as in a distinctly better fit in terms of agreement indices for $x = 0.267$ (see Tables 3 and 4), this was not the case for $x = 0.14$. Although the scattering contrast could be increased to ca 16 electrons when measuring only 8 eV away from the $Ta L_{III}$ absorption edge (rather than 1 electron contrast far from the edge), the low concentration of W in

$Ta_{74}W_6O_{203}$, which is only 7.5% compared with 15.2% in $Ta_{22}W_4O_{67}$, almost precludes a meaningful refinement of the occupational parameters $P_\mu(2q_M)$ and $P_\mu(4q_M)$. However, secondary evidence, i.e. bond-valence sums (Brown & Altermatt, 1985) as a function of $q \cdot t$ as well as the $q \cdot t$ dependence of the thermal parameter $U_{33}^M(q_M \cdot t_M)$, suggests the presence of a specific ordering pattern. This is the case even for the $x = 0.1$ sample, where $MoK\alpha$ data do not allow a differentiation of Ta and W on the basis of different atomic scattering factors, as will be shown below.

There is a discrepancy between the stoichiometries implied by full occupancy of all the refined atomic positions and those required by charge balance. It was suggested by Schmid et al. (1995) that the charge balance could be satisfied by taking into account anion vacancies at the O_M sites, i.e. the apical oxygen position (rather than to assume the presence of those vacancies in the basal plane as in Stephenson & Roth, 1971a,b,c,d). The refinement of the occupational modulation in $Ta_{22}W_4O_{67}$ reveals a pronounced preference for W at $q \cdot t = 0$ and $\frac{1}{2}$ (see Fig. 3). These points have a $(4 + 2)$-fold coordination, as pointed out in §5.3, and correspond to positions $M1$ and $M7$ in Schmid et al. (1995). The same result is obtained for $Ta_{74}W_6O_{203}$, although less significantly for reasons discussed already. The plot of the thermal parameter component $U_{33}^M(q_M \cdot t_M)$ (see Fig. 4) shows a striking similarity to the occupational modulation, as does the average bond-valence sum for the metal atom (see Fig. 5). The Ta/W ratio in all three compounds requires that the metal-atom positions corresponding to $q \cdot t = 0$ and $\frac{1}{2}$ are partially occupied by Ta. The bond valence sum depicted in Fig. 5,

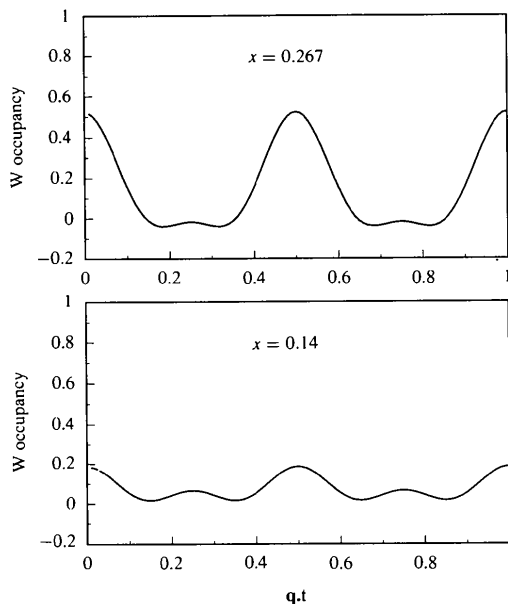however, indicates that the Ta would be strongly overbonded on those sites, unless one assumes an anion vacancy at one of the two adjacent O_M positions. This vacancy might occur at random either above or below the metal position. Yet it requires the Ta to adjust its valence by moving closer to the opposite apical O_M, resulting in a smeared out mean square displacement on the octahedral $(4 + 2)$ sites. This is reflected by the prominent modulation of $U_{33}^M(q_M \cdot t_M)$ found for all three compounds, indicating maximum displacement at $q \cdot t = 0$ and $\frac{1}{2}$, while being distinctly lower at the positions in between.

The bond-valence sum (Brown & Altermatt, 1985) of the tungsten-bearing metal-atom positions is determined by the Ta to W ratio, since the refined geometry necessarily represents an averaged coordination polyhedron. Thus, the decrease in tungsten content on going from $x = 0.267$ to 0.1 results in a diminishing bond-valence sum for the metal-atom positions at $q \cdot t = 0$ and $\frac{1}{2}$ (see Fig. 5). Moreover, the diminishing W content requires the concentration of oxygen vacancies to increase for mere charge balance. The assumption that
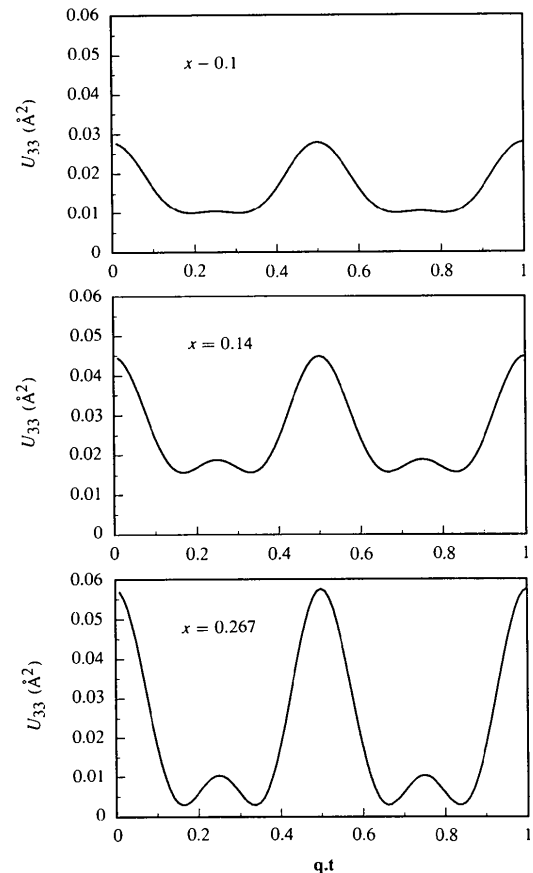

Fig. 3. Occupational modulation of tungsten as a function of $q_M \cdot t_M$.

Fig. 4. U_{33} component of the thermal parameter atomic modulation function of the metal atoms for different compositions.

the vacancies occur only at the apical positions would obviously imply an increasing mean-square displacement along c, i.e. $U_{33}^M(q_M \cdot t_M)$, for the metal atoms with increasing vacancy concentration. This is not consistent with the trend observed experimentally (see Fig. 4). For the oxygen vacancies to occur elsewhere, either exclusively in the basal plane or on both the apical position and in the basal plane, would require the presence of disorder in the basal plane. However, the thermal parameters $U_{11}^M(q_M \cdot t_M)$, $U_{22}^M(q_M \cdot t_M)$ of the metal atoms give no evidence for such a vacancy distribution. At this stage a vacancy distribution model has yet to be developed, which overcomes the apparent contradiction between the bond-valence requirements of the metal atoms and the thermal parameter modulation trend.

5.5. What is wrong with the first-order satellites?

The unsatisfactory fit to the first-order satellite reflections, quite pronounced in the present $x = 0.1$ refinement, is a feature observed in all the refinements, with a decreasing fit on going from $x = 0.267$ to 0.1.
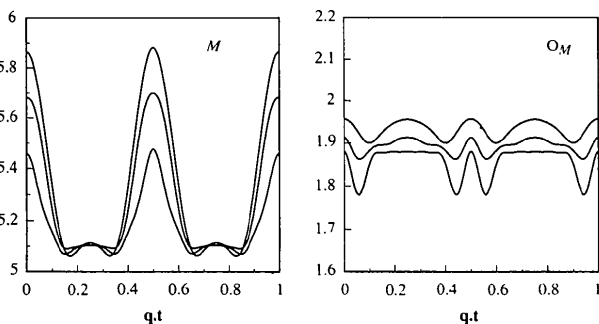

Fig. 5. Average bond-valence sum of the metal atom and oxygen O_M as a function of $q_M \cdot t_M$ for different compositions.

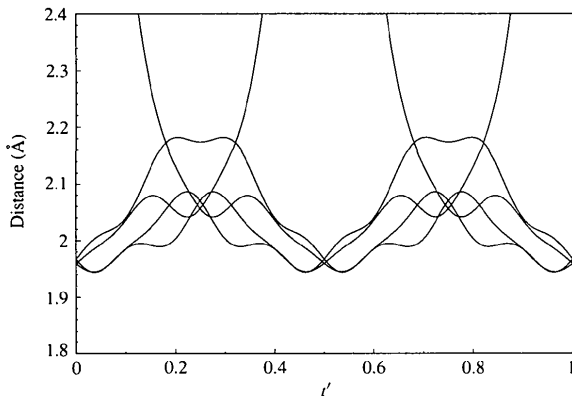Fig. 6. Metal–oxygen distances in the basal plane as a function of $t' = q_M \cdot (t_M - t_O)$.

Rae, Schmid, Thompson, Withers & Ishizawa (1995) were also aware of this problem.

Part of the problem in the case of $x = 0.1$ can probably be attributed to the lower quality of the measured data. The R value on merging symmetry-equivalent reflections (see Table 2) is surprisingly worse for the first-order satellite reflections compared with second and third order, although they are on average comparable in intensity. Although reflections obviously affected by resolution problems owing to the chosen X-ray wavelength were excluded from the refinement, erroneous reflections were probably not thoroughly avoided. This, of course, does not account for the trend across the composition range.

While the systematic extinction conditions unequivocally indicate the $\{\sigma_x|0,0,0,\frac{1}{2}\}$ symmetry operation to be present, lowering of the symmetry to the $C'm$--$(0\beta0)s$-- subgroup of $C'mmm(0\beta0)s00$ is still conceivable and would allow c-axis 'motion' otherwise forbidden by the $\{\sigma_z|0,0,0,0\}$ symmetry operation. A refinement in e.g. $C'mm2(0\beta0)s00$ was able to lower the residual values (although only marginally), however, yielding the same unsatisfactory pattern of R values for the different satellite orders, while giving no significant evidence for long-range c-axis 'motion'. Therefore, we consider our structural model and its attributed symmetry to be correct as far as long-range order is concerned. TEM exposures of the [100] zone axis and others revealed the presence of considerable diffuse intensity (see Fig. 7 in Schmid, Withers & Thompson, 1992), which becomes more structured and more pronounced, although not necessarily stronger in terms of integrated intensity, on going from $x = 0.267$ to 0.1. This sharpening in the diffuse pattern apparently correlates to the worsening fit of the first-order satellites.

6. Concluding remarks

The structure refinement of $(1-x)Ta_2O_5.xWO_3$, $x = 0.1$, as an incommensurately modulated composite structure, while giving a result consistent with the previously reported structural analysis of $Ta_{22}W_4O_{67}$ and $Ta_{74}W_6O_{203}$ (Schmid et al., 1995; Rae, Schmid, Thompson, Withers & Ishizawa, 1995), revealed subtle but significant differences across the solid solution. Some of these differences are present in the data reported earlier (Schmid et al., 1995; Rae, Schmid, Thompson, Withers & Ishizawa, 1995), but could not be interpreted in terms of a systematic composition-dependent change. Firstly, the present structural analysis showed a continuous variation of the b component of the AMF of atom O_M from a sinusoidal to a saw-tooth shape. Secondly, it clearly demonstrated the decrease of the bond-valence sum of the metal atoms at $q \cdot t = 0$ and $\frac{1}{2}$ with decreasing tungsten content. Thirdly, the mean-square displacement along c of the metal atoms is shown to diminish with decreasing W content.

The present refinement also helped to identify apparent deficiencies of the previously reported crystallographic model. Short-range order seems to be crucial for a more comprehensive understanding of the behaviour of the structure as a function of composition. This will require additional structural information not provided by X-ray Bragg intensities, but available in the diffuse intensity.

References

Brown, I. D. & Altermatt, D. (1985). *Acta Cryst.* B41, 244–247.

Fütterer, K., Schmid, S., Thompson, J. G., Withers, R. L., Ishizawa, N. & Kishimoto, S. (1995). *Acta Cryst.* B51, 688–697.

Grigg, M. W. & Barnea, Z. (1993). *Software Amendments for Philips PW1100/20.* School of Physics, University of Melbourne, Melbourne, Australia.

Hall, S. R. & Stewart, J. M. (1990). Editors. *Xtal3.0 Reference Manual.* Universities of Western Australia, Australia, and Maryland, USA.

Janner, A. & Janssen, T. (1980). *Acta Cryst.* A36, 399–415.

Petrícek, V. (1994). *JANA94. Programs for Modulated and Composite Crystals.* Institute of Physics, Praha, Czech Republic.

Rae, A. D. (1994). *RAELS94. A Comprehensive Constrained Least Squares Refinement Program.* Research School of Chemistry, Australian National University, Canberra, Australia.

Rae, A. D., Schmid, S., Thompson, J. G., Withers, R. L. & Ishizawa, N. (1995). *Acta Cryst.* B51, 709–721.

Schmid, S. & Withers, R. L. (1995). *Acta Cryst.* B51, 746–753.

Schmid, S., Thompson, J. G., Rae, A. D., Butler, B. D., Withers, R. L., Ishizawa, N. & Kishimoto, S. (1995). *Acta Cryst.* B51, 698–708.

Schmid, S., Withers, R. L. & Thompson, J. G. (1992). *J. Solid State Chem.* 99, 226–242.

Smaalen, S. van (1991). *Phys. Rev. B*, 43, 11330–11341.

Smaalen, S. van (1994). *MISTEK. Calculation and Plotting of Interatomic Distances, Angles, Occupation Probabilities and Bond-Valences for Intergrowth or Misfit Compounds and Incommensurately Modulated Structures.* Laboratory of Chemical Physics, University of Groningen, Groningen, The Netherlands.

Stephenson, N. C. & Roth, R. S. (1971a). *Acta Cryst.* B27, 1010–1017.

Stephenson, N. C. & Roth, R. S. (1971b). *Acta Cryst.* B27, 1018–1024.

Stephenson, N. C. & Roth, R. S. (1971c). *Acta Cryst.* B27, 1031–1036.

Stephenson, N. C. & Roth, R. S. (1971d). *Acta Cryst.* B27, 1037–1044.

Yamamoto, A. (1992). *Acta Cryst.* A48, 476–483.

Yamamoto, A. (1993). *Acta Cryst.* A49, 831–846.